Surface Wave Propagation in Thin Silver Films under Residual Stress

A. Njeh[a,b], T. Wieder[b], D. Schneider[c], H. Fuess[b], and M. H. Ben Ghozlen[a]

[a] Science Faculty, Department of Physics, Ultrasonic Laboratory, Sfax University, 3018 Sfax, Tunisia

[b] University of Technology Darmstadt, Institute for Materials Science, Petersenstr. 23, D-64287 Darmstadt, Germany

[c] Fraunhofer-Institut für Material- und Strahltechnologie, Winterbergstr. 28, D-01277 Dresden Germany

Reprint requests to A. N., Fax: +216-74-274437, E-mail: njeh@yahoo.com

Z. Naturforsch. **57 a,** 58–64 (2002); received December 7, 2001

Investigations using surface acoustic waves provide information on the elastic properties of thin films. Residual stresses change the phase velocity of the surface waves. We have calculated the phase velocity and dispersion of surface waves in thin silver films with a strong [111]-fibre texture. A non-linear description of surface waves propagating along the [110]-direction of the substrate has been developed on the basis of an acoustoelastic theory, taking into account residual stresses. The relative change $\Delta v/v$ of the velocity v was found to be linear for large excitation frequencies. The dispersion curves were measured using a photoacoustic method. For sputtered polycrystalline thin silver films we found good agreement between the experimental and calculated dispersion curves for frequencies up to 225 MHz.

Key words: Ultrasonic Surface Waves; Photoacoustic; Thin Films; Residual Stress; Texture.

1. Introduction

The velocity v of elastic waves (ultrasonic waves) within a medium depends on residual stress. The relative change $\Delta v/v$ of the wave velocity v of the unstressed medium is of the order of $\Delta v/v$ = 0.02. The acousto-elastic theory relates the velocity change to residual stresses for waves within a bulk medium. For that particular case, Cauchy formulated a continuum theory of small disturbances (ultrasonic waves) superimposed on an elastically deformed body, as described in [1]. Hayes and Rivlin [2] were the first to develop a theory for surface waves in homogeneously deformed elastic materials. They considered waves propagating in the direction of one of the principal stress axes. Their treatment has been generalized by Iwashimizu and Kobiri [3] to the case in which the propagation direction does not coincide with one of the principal stress axes. In all these treatments the material was assumed to be isotropic. Many materials commonly used in technology are, however, anisotropic in nature. The behavior of isotropic and anisotropic thin films has been treated by Farnell and Adler [4].

Surface acoustic waves (SAW) are a convenient tool to study the mechanical properties and the stress states of thin films, as they penetrate the material only down to a depth of approximately one wavelength [5]. The purpose of this paper is to apply the theory proposed by Farnell and Adler to thin silver films on (001) silicon substrates in order to describe the effect of the residual stress on the surface wave propagation along these films. We consider the residual stress as a perturbation on the surface wave propagation [6]. Our theoretical results are compared with observed experimentally data. By X-ray diffraction measurements, residual stress has been detected in silver films deposited by sputtering.

2. X-ray Analysis of Thin Silver Films

2.1. Deposition

Using dc-magnetron sputtering, four polycrystalline silver films were deposited on (001) Si substrates. Prior to the film growth, the chamber was evacuated to a pressure of 10^{-7} mbar. Then argon gas was introduced up to a pressure of 0.01 mbar.

The Ag target had a purity better than 99.9%. Prior to deposition, the target was pre-sputtered for 5 min with the substrate shutter closed. They were ultrasonically cleaned by isopropanol and deionized water and finally dried with pressurized nitrogen gas. The resulting Ag films had a thickness of about 102 nm.

2.2. *Texture and Elastic Constants*

X-ray measurements were performed on a texture diffractometer Seifert PTS 3003 with CuK_α radiation. For each film, three pole figures for the (111), (200) and (220) lattice planes were recorded. For a complete texture description, the pole figures must be transformed into an orientation distribution function (ODF). The ODF was derived through the application of the computer program BEARTEX [7] and revealed an orientation of the (111) planes parallel to the sample surface for the majority of the crystallites. The film crystallites are oriented along the [111] axis with isotropic distribution.

The investigation of surface acoustics waves requires the values of the elastic coefficients. Since the crystallite dimensions are small compared to the ultrasonic wavelength, the effective rigidity tensor may be considered as the average of the rigidity tensor of all crystallites with the [111] three-fold Ag symmetry axis parallel to the surface normal. This approach was previously used to evaluate the rigidity tensor of polycrystalline materials [8, 9]. In the framework of this assumption, the coefficients of the elastic tensor for silver are: $\tilde{c}_{11} = \tilde{c}_{22} = 152.8$ (GPa), $\tilde{c}_{33} = 162.73$ (GPa), $\tilde{c}_{12} = 82.07$ (GPa), $\tilde{c}_{13} = \tilde{c}_{23} = 72.13$ (GPa), $\tilde{c}_{44} = \tilde{c}_{55} = 25.43$ (GPa) and $\tilde{c}_{66} = (\tilde{c}_{11} - \tilde{c}_{12})/2$. These coefficients are defined in a coordinate system (x_1, x_2, x_3) with x_3 perpendicular to the Ag/Si(001) interface and x_1, x_2 belonging to the interface. An elasticity tensor with the above relations among its components has the symmetry of a transverse isotropy crystal class [10].

2.3. *Stress*

Residual stress evaluation (RSE) by grazing incidence X-ray diffraction has been described by several authors [11 - 14]. Measurements have been carried out on four different Ag films, and we obtained on average a strain tensor with components $\varepsilon_{11} = 3.5 \times 10^{-3} \pm 0.8 \times 10^{3}$, $\varepsilon_{22} = 5.5 \times 10^{-3} \pm 0.8 \times 10^{-3}$, $\varepsilon_{33} = -0.9 \times 10^{-3} \pm 0.3 \times 10^{-3}$. These values were subsequently used in the ultrasonic surface wave analysis.

3. Ultrasonic Surface Wave Analysis

An ultrasonic surface wave propagates at the surface of a homogenous material with amplitude that decreases exponentially perpendicular to the surface and vanishes to negligible values within a few wavelengths below the surface. If the frequency is increased, then the penetration depth decreases. The velocity of propagation is somewhat less than the bulk shear velocity associated with the material, which is the same for all frequencies. If the material is coated with a film, which has different elastic parameters, then the surface wave becomes dispersive. The wave with higher frequency has a lower penetration depth and is more influenced by the film than the wave with lower frequency.

3.1. *Displacement Field*

The coordinate system used in the present calculations is given in Figure 1. Here, the plane with $x_3 = 0$ is the interface between the layer and the substrate, while $x_3 = h$ is the free surface. The propagation direction of the ultrasonic surface wave is taken along the x_1 axis. The wave must satisfy both the appropriate wave equation in the layer and the substrate as well as the boundary conditions imposed by the interface and the free surface. The wave equation for the particle displacements in a perfectly elastic and homogeneous medium can be written, in the absence of body forces and piezoelectric effects, as [15]

$$\rho \frac{\partial^2 u_i}{\partial t^2} = C_{ijkl} \frac{\partial^2 u_l}{\partial x_j \partial x_l}, (i, j, k, l = 1, 2, 3), \quad (1)$$

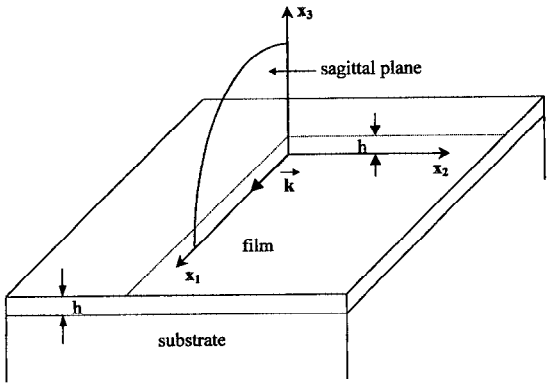

Fig. 1. Coordinate system for surface acoustic waves propagating in a thin film.

in which ρ is the density of the medium and C_{ijkl} the elastic tensor. Each component in (1) is referred to the coordinate system of Fig. 1 and the summation convention on repeated subscripts is implied.

In the following, a quantity carrying a tilde designates a quantity of the film, and the same quantity without a tilde refers to the substrate. Thus $\tilde{\rho}$ and $\tilde{C}_{ijkl}$ are the density and the elastic tensor of the layer material and ρ and C_{ijkl} are the density and the elastic tensor of the substrate. We assume a straight crested surface wave propagating in the x_1 direction with

$$u_j = u_{0j} \exp(ik\beta x_3) \exp[ik(x_1 - vt)], \qquad (2)$$

where k is the wave vector, v the propagation speed and β a complex constant. A surface wave is proposed to be a linear combination of partial inhomogeneous plane waves of the form of (2), which satisfy the motion (1) and certain boundary conditions.

In order to have a nontrivial displacement, u_j, β and v must satisfy the characteristic equation

$$|\Gamma_{il} - \delta_{il}\rho v^2| = 0, (i, l = 1, 2, 3), \qquad (3)$$

where

$$\Gamma_{il} = C_{ijkl} n_j n_k \qquad (4)$$

is the Christoffel tensor and n_j, n_k are the components of the vector $\vec{n}(1, 0, \beta)$. For a given v, (3) is an equation of order 6 in β and may be solved for the six roots $\beta^{(n)}$ (n = 1 to 6). The six roots for β are either real or occur in complex conjugate pairs. All six roots are used for the calculation of the film displacement, but only the three roots with positive imaginary parts are taken for the substrate displacement. For the textured Ag film, the interface plane, i. e. $x_3 = 0$, is isotropic. The elastic tensor for our Ag films is that given in Section 2.2. The components of the Christoffel tensor (4) under the assumption of transverse isotropy symmetry (see Section 2.2) are

$$\tilde{\Gamma}_{11} = \tilde{c}_{55}\tilde{\beta}^2 + \tilde{c}_{11}, \tilde{\Gamma}_{22} = \tilde{c}_{44}\tilde{\beta}^2 + \tilde{c}_{66},$$

$$\tilde{\Gamma}_{33} = \tilde{c}_{33}\tilde{\beta}^2 + \tilde{c}_{55}, \tilde{\Gamma}_{13} = (\tilde{c}_{55} + \tilde{c}_{13})\tilde{\beta}, \tilde{\Gamma}_{12} = \tilde{\Gamma}_{23} = 0.$$

Writing the displacements as a linear combination of terms having the phase velocity v, the displacement field in the layer is given as

$$\tilde{u}_j = \Big[\sum_n \tilde{A}_n \tilde{u}_{0j}^{(n)} \exp(ik\beta^n x_3)\Big] \cdot \exp[ik(x_1 - vt)], \qquad (5)$$

$$n = 1 \text{ to } 6,$$

and in the substrate as

$$u_j = \Big[\sum_n A_m u_{0j}^{(m)} \exp(ik\beta^m x_3)\Big] \cdot \exp[ik(x_1 - vt)],$$

$$m = 1, 3, 5, \qquad (6)$$

The coefficients A_m with even subscript m are omitted because they are not related to finite solutions. $\tilde{u}_{0j}^{(n)}$ and $u_{0j}^{(m)}$ are the complex eigenvectors associated with the characteristic equation (3) for the film and for the substrate. $\tilde{A}_n$ and A_m are the weighting factors for the linear combination of waves in the film (5) and the substrate (6). Only one eigenvector exists for each root β. $\tilde{u}_{0j}^{(n)}$ and $u_{0j}^{(m)}$ are the components of the eigenvector corresponding to the eigen values $\tilde{\rho}v^2$ and ρv^2, respectively. The weighting factors must be determined by the application of the boundary conditions based on the displacements in (5) and (6). The particle displacements and the traction components caused by the stress components of the wave (T_{13}, T_{23}, and T_{33}) must be continuous across the interface under the assumption of a rigid contact between the two materials. Since the free surface is considered to be mechanically stress free, the three traction components of stress must vanish thereon and nine boundary conditions are obtained. In order to obtain nontrivial solutions of this set of homogenous equations, the 9×9 determinant of the coefficients $\tilde{A}_n$ and A_m must vanish.

For the substrate, the wave vector will be defined as x_1 = [110] direction. The elastic coefficients for Si with respect to the crystallographic axes are given in [10]. After transforming to the sample system (x_1, x_2, x_3) with x_3= [001], the coefficients are c_{11} = 194.25 (GPa), c_{33} = 165.6 (GPa), c_{12} = 35.7 (GPa), c_{13} = 63.9 (GPa), c_{44} = 79.53 (GPa) and c_{66} = 51.3 (GPa). It is obvious that the Christoffel tensor for the substrate has the same form as for the silver film, since the components $\Gamma_{12} = \Gamma_{23} = 0$. The secular equation is therefore for both materials

$$[\Gamma_{22} - \rho v^2] \cdot [(\Gamma_{11} - \rho v^2) \cdot (\Gamma_{33} - \rho v^2) - \Gamma_{13}^2] = 0. \qquad (7)$$

This secular equation separates into two parts. The sagittal-plane displacements are completely uncoupled in the equations of motion from transverse displacements. The solutions can always be separated into two groups when the sagittal plane (x_1, x_3) fits with the Si symmetry plane. The first group of solutions has solely transverse displacements, which are

called Love modes. The other group has sagittal displacements, which are called Rayleigh modes. The boundary conditions can be satisfied with two kinds of solutions, those involving A_1, $\tilde{A}_1$, and $\tilde{A}_2$ (Love modes) and those involving A_3, A_5, $\tilde{A}_3$, $\tilde{A}_4$, $\tilde{A}_5$ and $\tilde{A}_6$ (Rayleigh modes). For both Love mode and Raleigh mode it is often convenient to obtain the dispersive curves by assuming fixed values of velocity v and then solving the boundary-condition equation by searching for a value of the product kh of the wave number k and film thickness h which vanishes the boundary condition determinant.

3.2. Dispersion

We apply the above theory to the Ag/Si system. First, we consider the system under residual stress and the results thus obtained will be compared with those for an unstressed film. We want to include the effect of residual stresses on the film's elastic constants $\tilde{c}_{ijkl}$. For this purpose we can apply a correction of the elastic coefficients given in [6] which depends on the residual strain tensor and hyper-elastic constants $\tilde{c}_{ijklmn}$. Assuming the same geometry, the elastic tensor $\bar{c}_{ijkl}$ including the stress effect is written as

$$\bar{c}_{ijkl} = \tilde{c}_{ijkl} + c^*_{ijkl}, \tag{8}$$

were $\tilde{c}_{ijkl}$ is the elastic tensor defined in the (x_1, x_2, x_3) coordinate system, and c^*_{ijkl} is the corresponding perturbative correction due to the initial deformation in the film.

The above calculation requires the knowledge of the hyper-elastic coefficients $\tilde{c}_{ijklmn}$ expressed in the (x_1, x_2, x_3) coordinate system. Values of $\tilde{c}_{ijklmn}$ are obtained by transforming the hyper-elastic coefficients of Ag single crystal [16] in the same way as for $\tilde{c}_{ijkl}$ (see Sect. 2). Consequently, the effective elastic coefficients (denoted by the bar) for the film are: $\bar{c}_{11}$ = 149.8 (GPa), $\bar{c}_{33}$ = 154.1 (GPa), $\bar{c}_{12}$ = 80.4 (GPa), $\bar{c}_{13}$ = 73.9 (GPa); $\bar{c}_{23}$ = 74.2 (GPa) and $\bar{c}_{44}$ = 24.1 (GPa).

At this point, the elastic constants of both film and substrate are available with respect to the same coordinate system (x_1, x_2, x_3). Then one can solve the equation of motion (1) and deduce the sixth order secular equation. The results thus obtained are separated into two sets: Love modes; which are polarized perpendicular to the sagittal plane (x_1, x_3), and Rayleigh modes, polarized inside the sagittal plane.

3.2.1. Love modes

For a given velocity v, the resolution of the characteristic equation, $[\Gamma_{22} - \rho v^2] = 0$, and the boundary conditions determinant has multiple solutions in kh. We have found that the Love modes can propagate only if $\bar{v}_s < v_L < v_s$, respectively $\tilde{v}_s < v_L < v_s$. From the elastic constants for film and substrate we calculated values for the shear velocity ($v = (c_{66}/\rho)^{1/2}$) in the substrate, the stressed Ag film, and the unstressed Ag film: v_s = 4692 m/s, $\bar{v}_s$ = 1786 m/s and $\tilde{v}_s$ = 1836 m/s. Since Love modes are dispersive, it can be checked that for $h \ll \lambda$ ($hk \to 0$) v_L becomes very close to v_s. The other case corresponds to $h \gg \lambda$ ($hk > 1$). Under this condition v_L is close to $\bar{v}_s$ (respectively $\tilde{v}_s$). The calculated values of the shear wave velocity along the silver film make up a difference which can be experimentally confirmed in measurements at high frequencies.

3.2.2. Rayleigh modes

For each material, the same approach as discussed above leads to fourth order characteristic equations. Besides, the remaining boundary conditions relative to displacements and stress tensor components reveal kh solutions of Rayleigh modes. Concentrating on the first Rayleigh mode, it can be seen that the velocity varies between v_R = 5080 m/s and $\tilde{v}_R$ = 1588 m/s. These two values are associated to the Rayleigh velocity, respectively, in Si and Ag. The residual stress changes the Ag Rayleigh velocity from $\tilde{v}_R$ to $\bar{v}_R$ = 1518 m/s. The transition from the substrate velocity v_R to the film velocity $\bar{v}_R$ is accomplished by changing from small values for kh to higher values.

In order to examine the effect of residual strain on the ultrasonic surface waves propagation we present for both modes (Rayleigh and Love) the relative velocity change $\Delta v/v$ as a function of kh (Fig. 2). The effect becomes more important for high values of kh ($\Delta v_R/v_R \cong 4.5\%$ and $\Delta v_L/v_L \cong 2.5\%$ for kh = 8 rd). Unfortunately, these frequency regions are not accessible with our experimental facility. Our ultrasonic measurements have been carried out up to frequencies of 250 MHz, which correspond to a value for kh of ≈ 0.1 rad.

Being interested in the first Rayleigh mode for frequencies up to 225 MHz, we calculated theoretical dispersion curves for this frequency range. Figure 3 shows the relative change $\Delta v_R/v_R = 2 \cdot [v_R$ (unstrained film) – v_R (strained film)] / [v_R (unstrained

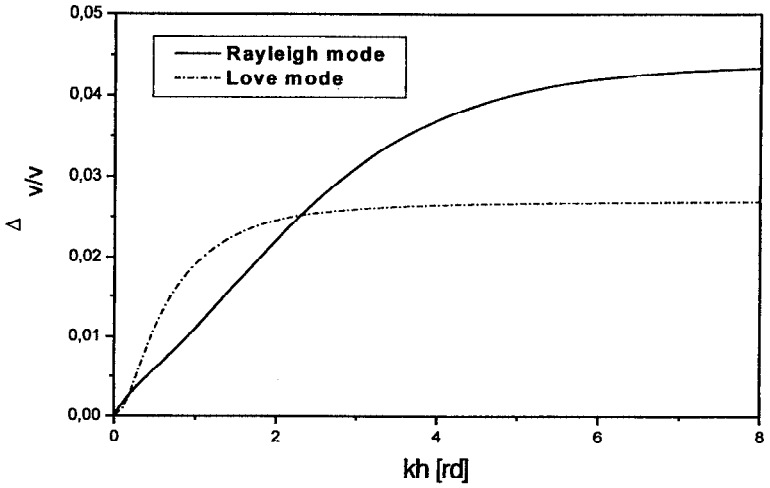

Fig. 2. $\Delta v/v$ curves as functions of the product kh of the wave number k and the film thickness h for the two surface waves (First Love mode and first Rayleigh mode).

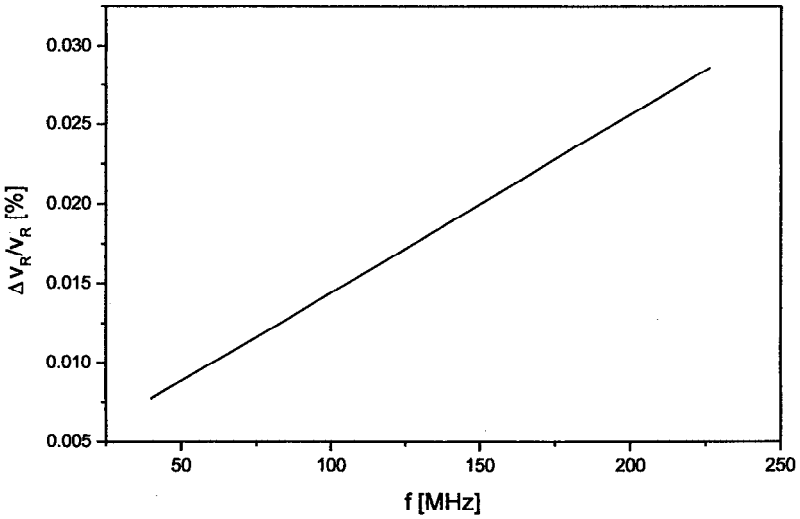

Fig. 3. Relative change $\Delta v_R/v_R = 2 \cdot [v_R$ (unstrained film) $- v_R$ (strained film)] / [v_R (unstrained film) + v_R (strained film)] between the two theoretical dispersion curves v_R (unstrained film) and v_R (strained film) for the first Rayleigh mode of an Ag thin film.

film) + v_R (strained film)] between the two theoretical dispersion curves v_R (unstrained film) and v_R (strained film) for the first Rayleigh mode of a thin Ag film. The observed relative shift $\Delta v/v$ varies from 0.004% for 40 MHz up to 0.028% for 225 MHz. It appears that for high frequencies the Rayleigh wave has a lower penetration and is more intensively influenced by the residual strain. Compared to bulk acoustic waves, the surface wave generates a relative velocity change sensitive to the wave frequency.

4. Ultrasonic Measurements

In Fig. 4, the laser ultrasonic experimental equipment utilized for this study is shown. This device has been developed in the Fraunhofer-Institut for Material and Beam Technology, Dresden, Germany [17]. Short pulses (pulse duration: 0.5 ns, energy: 0.4 mJ) of a nitrogen laser are focused by a cylindrical lens on the surface of the sample and generate wide-band surface wave pulses. The SAW pulses are detected by wide-band a piezoelectric transducer (bandwidth: 250 MHz). Specimen and transducer are fixed to a translation stage that moves perpendicular to the position of the laser beam to vary the distance d between the laser focus line and the transducer. The surface acoustic waveform is detected at different distances d_1 and d_2. A Fourier transform of the waveform yields the phase spectra ϕ_1(f) and ϕ_2(f). The wave velocity v_R, depending on the frequency f, is determined by

$$v_R(f) = \frac{2\pi f(d_2 - d_1)}{\phi_1(f) - \phi_2(f)}. \tag{9}$$

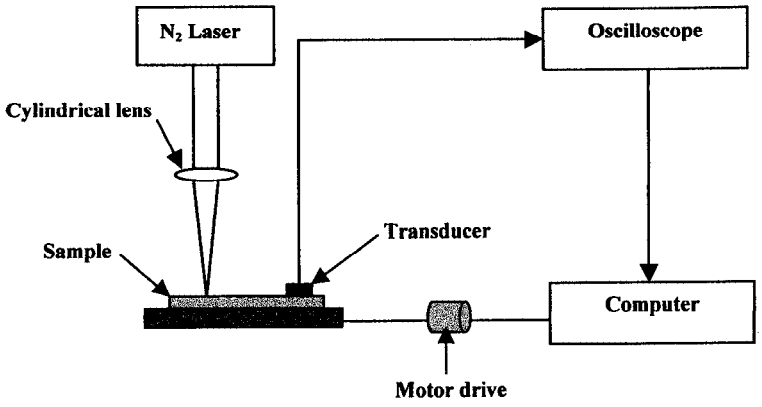

Fig. 4. Experimental set-up of the photoacoustic equipment.

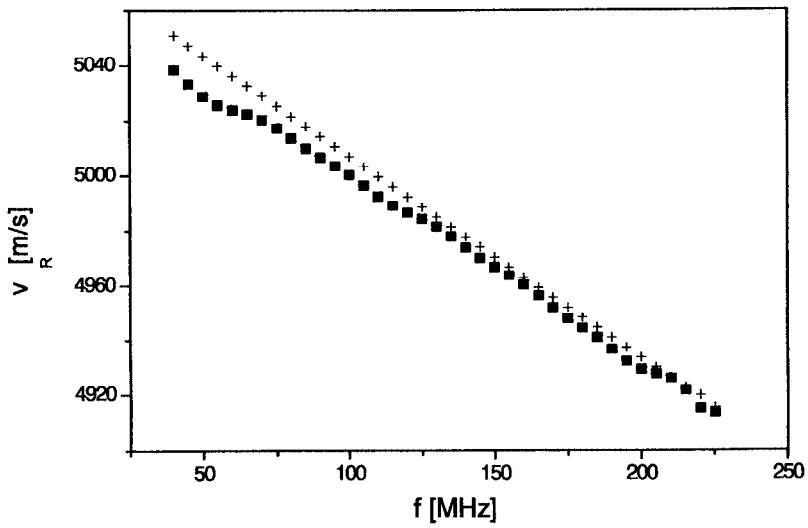

Fig. 5. Measured Dispersion curve of the first Rayleigh mode (squares) and the corresponding calculated dispersion curve (crosses).

The experimentally observed dependence of the wave velocity v_R of the first Rayleigh mode on the frequency f is shown by the squared symbols in Figure 5. The theoretical results of the Rayleigh mode dispersion of the strained Ag film are presented by the crossed symbols in Figure 5. The frequency increases up to 225 MHz. In this range (from 40 MHz to 225 MHz) one can determine the elastic properties of films with a thickness down to 100 nm [17 - 21]. For frequencies above $\approx$ 125 MHz, the experimental results agree with the theoretical results mentioned above. One can introduce a deviation parameter δ, as defined below, to quantify the difference between experimental and theoretical results, according to

$$\delta = 2 \sum_{i=1}^{N} \frac{v_R^{calc}(i) - v_R^{mes}(i)}{v_R^{calc}(i) + v_R^{mes}(i)}, \qquad (10)$$

where i represents the discrete non-dimensional wave number, N is the number of data points used, v_R^{mes} the measured Rayleigh mode velocity and v_R^{calc} the calculated one. For a frequency up to 225 MHz and for 6109 data points, the deviation parameter e is close to 0.12%. It is noted that the experimental results agree with the theoretical predictions, in particular at higher frequencies. The SAW analysis may be improved in the low frequency area if we take the orientation distribution function of the silver crystallites into account.

5. Conclusions

Theoretical calculations and experimental investigations of surface acoustic waves (SAW) have been carried out in polycrystalline, textured Ag films under residual stress. Applying the model of Farnell and Adler, we have obtained the dispersion curves of the surface waves. Theoretical analysis shows the importance of the effect of the residual stress on the

phase velocity at high frequencies. The shift of the Love mode velocity becomes very close to 0.025 for kh values up to 3 rd. For the Rayleigh mode, the velocity change increases with frequencies, but it remains small ≈ 0.0003 for an excitation frequency up to 225 MHz. Since $h \approx 10^{-7}$ m, in the product kh of the wave number k and the film thickness h, an usual ultrasonic excitation frequency of 225 MHz does not allow to enter regions of kh, where the effect of residual stresses is observable by SAW experiments.

Acknowledgement

One of us (A. N.) is grateful to a grant from the Deutscher Akademischer Austauschdienst (DAAD).

[1] P. P. Delsanto and A. V. Clark Jr., J. Acoust. Soc. Amer. **81**, 952 (1987).
[2] M. Hayes and R. S. Rivlin, Arch. Rational Mech. and Anal. **8**, 358 (1961).
[3] Y. Iwashimizu and O. Kobori, J. Acoust. Soc. Amer. **48**, 910 (1978).
[4] G. W. Farnell and E. L. Adler, Phys. Acoust. **9**, 35 (1972).
[5] M. Duquennoy, M. Ouaftouh, and M. Ourak, Nondestructive Testing and Evaluation **32**, 189 (1999).
[6] A. D. Degtyar and S. I. Rokhlin, J. Appl. Phys. **78**, 1547 (1995).
[7] H.-R. Wenk, S. Matthies, J. Donovan, and D. Chateigner, J. of Appl. Crystallogr. **31**, 262 (1998).
[8] T. Wieder, J. of Appl. Phys. **78**, 838 (1995).
[9] J. Zendehroud, T. Wieder, and H. Klein, Materialwissenschaft und Werkstofftechnik **26**, 553 (1995).
[10] E. Dieulesaint and D. Royer, "Ondeélastiques dans les solides", vol. 1, Masson, Paris 1996.
[11] C. M. Brakman, J. Appl. Crystallogr. **16**, 325 (1983).
[12] S. Ejiri, T. Sasaki, and Y. Hirose, Thin Solid Films **307**, 178 (1997).
[13] T. Wieder, Computer Phys. Comm. **85**, 398 (1995).
[14] A. Njeh, T. Wieder, and H. Fuess, Powder Diffraction **15**, 211 (2000).
[15] T.-T. Wu and Y.-H. Liu, Ultrasonics **37**, 405 (1999).
[16] Landolt-Börnstein, Neue Serie, III 29/a: "Low Frequency Properties of Dielectric Crystals: Elastic Constants", Editor: D. F. Nelson, Springer-Verlag, Berlin 1992.
[17] D. Schneider and T. Schwarz, Surface and Coating Techn. **91**, 136 (1997).
[18] D. Schneider and B. Schultrich, Surface and Coating Techn. **98**, 962 (1998).
[19] D. Schneider, Th. Witke, Th. Schwarz, B. Schoeneich, and B. Schultrich, Surface and Coating Techn. **126** (2000).
[20] H. Coufal, K. Meyer, R.K Grygier, M. de Vries, D. Jenrich, and P. Hess, Appl. Phys. **A59,** 83 (1996).
[21] B. Schultrich, H-J. Scheibe, G. Grandremy, D. Drescher, and D. Schneider, Diamond and Related Materials **5**, 914 (1996).